*Optica Applicata, Vol. XI, No. 1, 1981*

# A digital Fabry–Pérot spectrometer for the use in studies of pressure broadening and shift of spectral lines*

ANDRZEJ BIELSKI, WACŁAW DOKURNO, EDMUND LISICKI
Institute of Physics, Nicholas Copernicus University, ul. Grudziądzka 5/7, 87-100 Toruń, Poland.

ZYGMUNT TURŁO
Nicholas Copernicus Astrophysical Center, Polish Academy of Sciences, Astrophysical Laboratory, ul. Chopina 12, 87-100 Toruń, Poland.

A pressure scanned spectrometer with a Fabry–Pérot etalon for weak line shape and shift investigation is described. In this instrument the spectrum can be scanned at a number of discrete equidistant points. The Jamin interferometer is coupled with a Fabry–Pérot chamber to control the pressure. The signal at each point of the line profile is integrated in an electronic counter. The operation of this instrument has been automatized. Samples of the results obtained by means of this spectrometer are also included.

## 1. Introduction

Studies of profiles of spectral lines emitted at very low perturbing gas pressures can provide valuable information about interatomic potentials. It must be emphasized, however, that in order to distinguish between different theoretical models it is necessary that the pressure broadening and shift coefficients be measured to an accurancy of $5.0 \times 10^{-8}$ cm$^{-1}$/Pa.

In a previous paper [1], a pressure scanned spectrometer with a Fabry–Pérot interferometer (FPI) has been described. It has been later used in our laboratory in studies of collision broadening of many spectral lines of neon [2–4] and the 535.0 nm line of thalium [5]. The spectrometer described in [1] was an analogue-digital instrument. This means that the signal from the Fabry–Pérot interferometer was recorded in a digital form using a photon counting technique, whereas in the pressure control system an analogue processing of the signal was applied.

The present paper describes an improved version of the spectrometer reported in [1]. This new spectrometer is entirely a digital instrument and, moreover, enables to perform simultaneously measurements of both

* This work was carried out on the Research Project M.R. I.5.

the profile and the shift of its maximum. This is an instrument with high sensitivity, high spectral resolution and linear dispersion. It may also be characterized as an instrument with full automation of line profile and shift measurements.

In the present spectrometer, similary as in the previous one, the optical path length between the plates of the Fabry–Pérot interferometer is changed by discrete steps by the change of the gas pressure in the interferometer chamber. To obtain a uniform and linear change of the optical path length a Jamin interferometer is connected to the Fabry–Pérot etalon. A photon counting technique [6] is used to achieve an optimal signal to noise ratio.

## 2. Optical system

The figure 1 shows a schematic diagram of the optical system of the spectrometer. The electromagnetic shutters $D_1$ and $D_2$ enable us to record the signal from the source $K_1$ under investigation (or from the source $K_1$ under investigation and the reference source $K_3$) alternately with the signal from the Jamin interferometer. The shutters $D_3$ and $D_4$ allow to record signal either from the source under investigation $K_1$ or from reference source $K_3$. The light beam from the source $K_1$ passes through the following

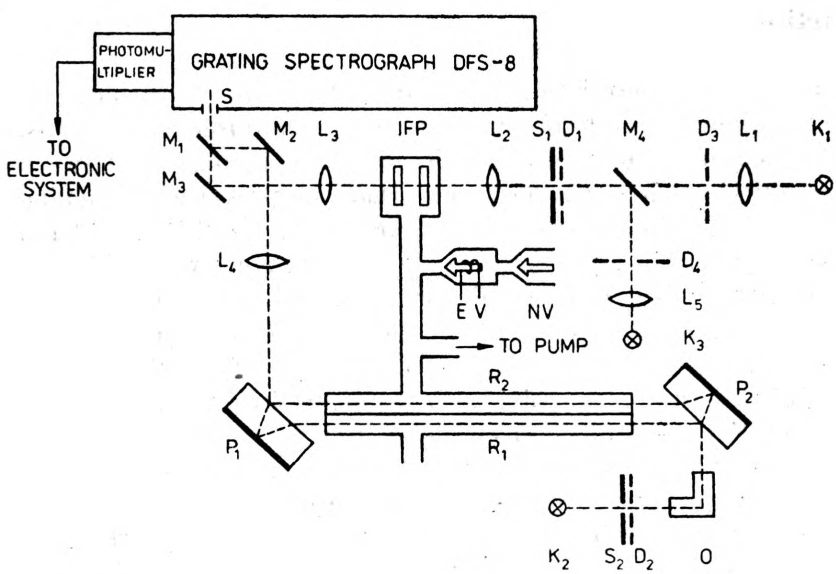


Fig. 1. Diagram of the optical system of the spectrometer

$M_1$ – $M_4$ mirors, $L_1$ – $L_5$ lenses, $S$ – $S_2$ slits, $D_1$ – $D_4$ shutters, FPI Fabry-Pérot etalon, EV electromagnetic valve, NV needle valve, $P_1P_2$ plates of Jamin interferometer, $R_1$,$R_2$ tubes of Jamin interferometer, $K_1$ – $K_3$ light sources system: the lens $L_1$, slit $S_1$, lens $L_2$, Fabry–Pérot interferometer, lens $L_3$, and is focussed on the entrance slit of the grating spectrograph DFS-8, which was used here as an entrance monochromator. The light from the reference source $K_3$ passes through the system: the lens $L_5$, the semi-transparent mirror $M_4$ and the slit $S_1$, lens $L_2$, FPI, lens $L_3$, and is focussed on the entrance slit of the monochromator.

The light beam from an auxiliary lamp $K_2$ passes through the slit $S_2$, concave spherical mirror $O$, the Jamin interferometer and the lens $L_4$ which gives an image of interference fringes on the entrance slit of the monochromator. In order to distinguish the light beams from Fabry–Pérot etalon and from the Jamin interferometer the entrance slit is fitted with a diaphragm of the form shown in fig. 2. The mirrors $M_1$ and $M_2$ are adjusted in such a way that the light from the Fabry–Pérot interferometer cannot pass through the upper part of the diaphram shown in fig. 2.

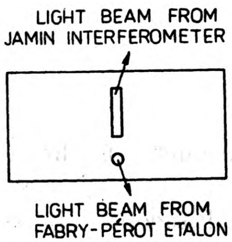


Fig. 2. Diaphgram at the entrance slit of the spectrograph

## 3. Data recording and pressure control system

In the spectrometer both the data recording and the pressure control are automatized. The instrument operates in two time sequences:

1. Recording of the signal from the Fabry–Pérot interferometer (coming from the source $K_1$ or $K_1$ and $K_2$) at discrete points of the line contour.

2. Change of the gas pressure in the Fabry–Pérot interferometer chamber and the Jamin interferometer producing discrete and equal increments of the optical path length.

The signal from the photomultiplier is detected using a photon counting technique by means of an electronic counter preceded by a preamplifier and a pulse normalization circuit.

The controlled change of the gas pressure in the chamber of the Fabry–Pérot interferometer is performed using the Jamin interferometer. In this interferometer there are two tubes $R_1$ and $R_2$ (see fig. 1), one of which is connected to the Fabry–Pérot interferometer chamber and the second one to the atmosphere. Figure 3 shows the dependence of the intensity of the light leaving the Jamin interferometer on the difference of the refraction index ($\Delta\mu$) of the air in the tubes $R_1$ and $R_2$.

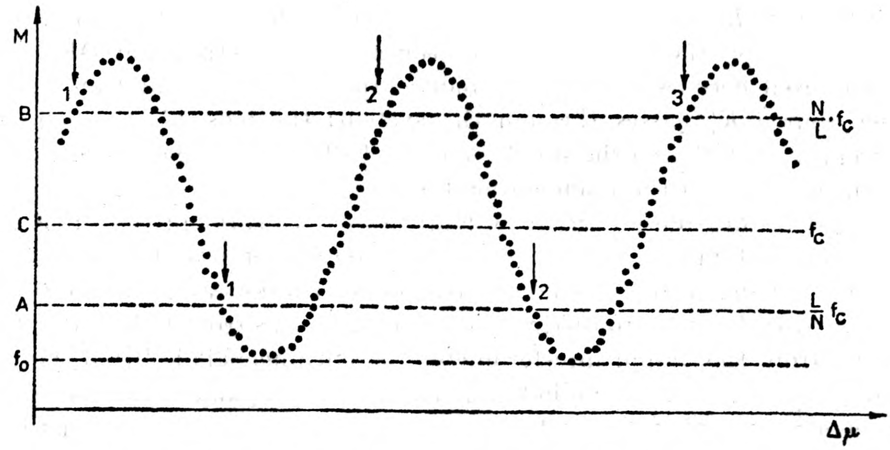


Fig. 3. Pulse frequency ($M$) from the Jamin interferometer as a function of refraction index $\Delta\mu$

For explanation see Appendix

## 4. Operation of the system

A block diagram of the electronic system of the spectrometer is shown in fig. 4.

I. The pulse "start" opens the shutter $D_1$ and simultaneously shuts the shutter $D_2$. At that time the shutter $D_3$ is open and the signal from the source $K_1$ under investigation is measured. The following operation are then performed:

1. A time delay (1s.) necessary to stabilization of shutters.
2. A counting of pulses from the photomultiplier (at a given time interval).
3. Print of the counter data on the printer.
4. Reset of the counter.

II. The next operation which is used in the measurements of the shift of the line profile maximum consists of two procedures: first the shutter $D_3$ is shut down and the shutter $D_4$ is opened and the signal from the reference sources $K_3$ is measured, then the shutter $D_3$ is opened and $D_4$ is shut down.

III. The third group of operations concern the change of the gas pressure in the Fabry–Pérot interferometer chamber. An electronic system which controls the operations of the counter creates a pulse in such a way that the shutter $D_1$ is shut down and the shutter $D_2$ is opened. The photomultiplier records then the light coming from the Jamin interferometer. After opening of the shutter $D_2$ electromagnetic valve EV is open and the pressure in the chamber of the Fabry–Pérot etalon as well as in the tube $R_2$ increases. At the moment when the value of the signal from the Jamin interferometer exceeds a certain determined value, let us say a level $B$ in fig. 3, a pulse is created which is responsible for following operations:

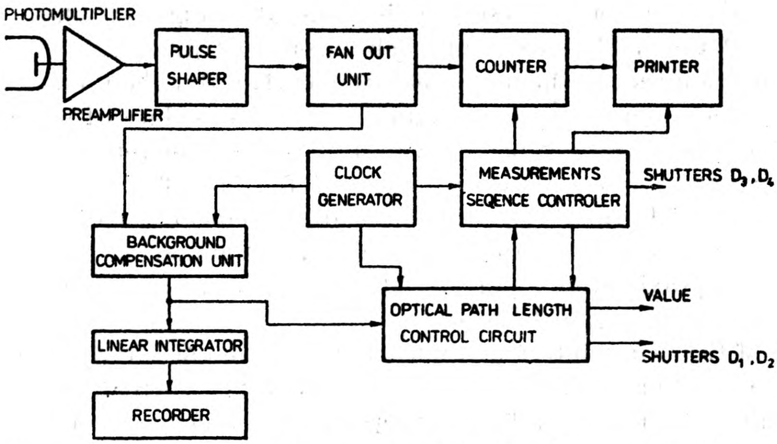


Fig. 4. Block diagram of the electronic system of the spectrometer

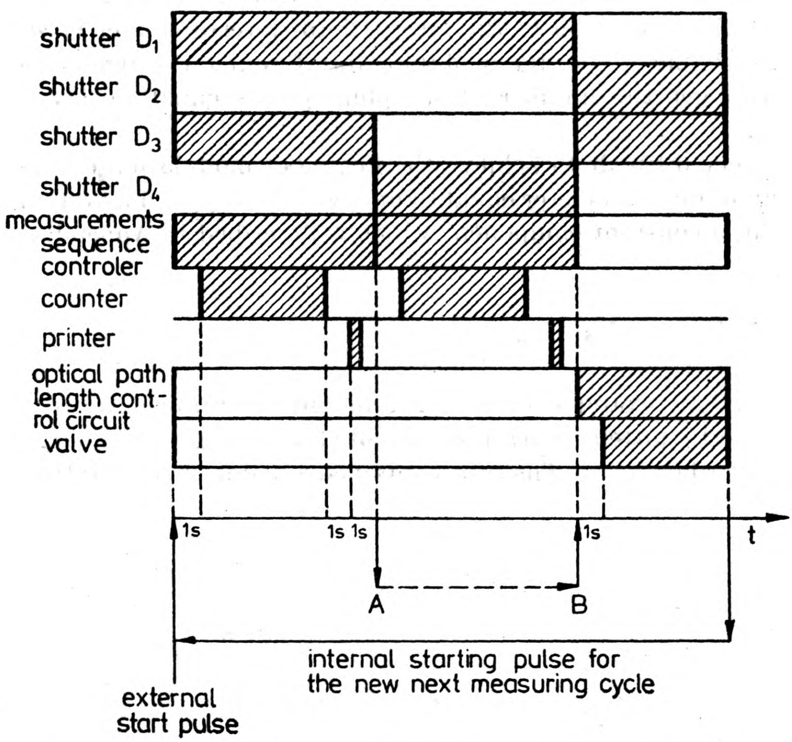


Fig. 5. Time sequence of the single measuring cycle of the spectrometer
Remark: if only the source $K_1$ is measured steps from $A$ to $B$ are omitted

1. Closing of the electromagnetic valve EV.
2. Closing of the shutter $D_2$.
3. Opening of the shutter $D_1$.
4. Generation of the pulse "start" which goes to the system controlling the counter, and begins a new measuring cycle in the spectrometer.

A pressure control system is described in Appendix. Figure 5 shows a time sequence of the single measuring cycle in our instrument.

We should mention that in the next measuring cycle (after the pressure control system is activated) the electromagnetic valve EV is shut off when the signal reaches the certain value $A$. This leads to the increments of pressure corresponding to the intervals $B_1A_1$, $A_1B_2$, etc. The changes of the refraction index $\Delta\mu$ caused by these pressure increments yield equal increments of the optical path length in the Fabry–Pérot etalon. The levels $A$ and $B$ are set approximately symmetrically with respect to the mean light intensity corresponding to the level $C$.

The number of the Jamin interferometer fringes within one interference order of the Fabry–Pérot interferometer is equal to $L/2t$, where $L$ is the length of the tubes $R_1$ and $R_2$ in Jamin interferometer and $t$ — distance between the plates of the Fabry–Pérot etalon. Since the electronic circuit yields two recordings for one Jamin interferometer fringe, the number of sampling points within one order of the Fabry–Pérot interferometer becomes equal to $L/t$. Using a counter of Jamin interferometer fringes (see Appendix) one can get the number of sampling points equal to $L/mt$, where $1 \leqslant m \leqslant 7$.

Because it is very difficult to achieve the degree of modulation of the light from the Jamin interferometer equal to one, we have applied a system of compensation of a constant component which is described in Appendix.

## 5. Examples of the results

The figure 6 shows an example of the interferogram obtained for the 582.02 nm line of Ne I emitted from a low current (1.45 mA) glow discharge tube of the type described in [2]. The tube contained a helium-neon mixture

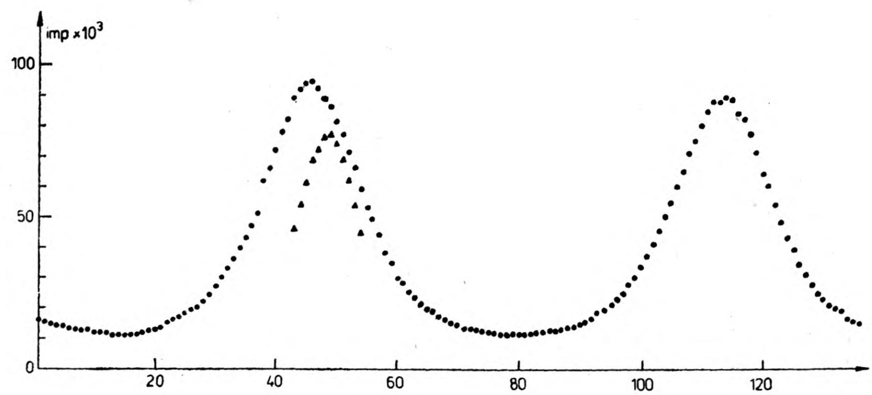


Fig. 6. Interferogram of the neon spectral line 582.02 nm perturbed by helium
● – experimental points of investigated light source ($K_1$), ▲ – experimental points of reference light source ($K_3$)

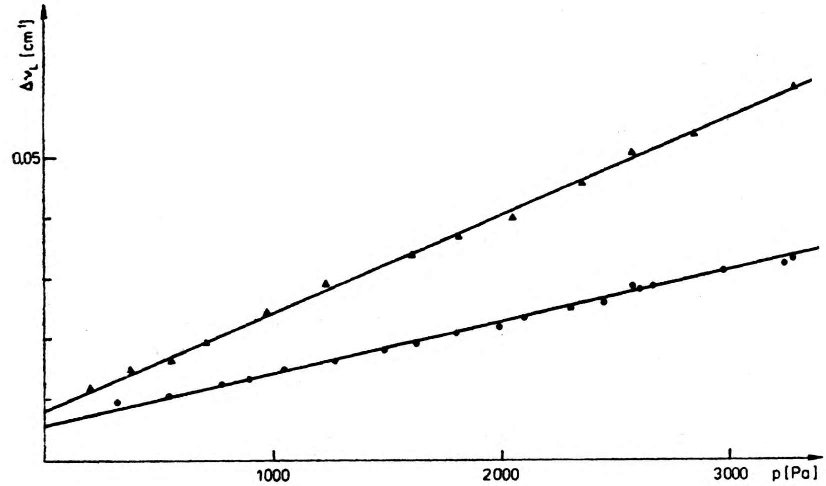


Fig. 7. Plot of the dependence of Lorentzian half-width on the neon pressure (● — experimental points) and helium pressure (▲ — experimental points) for the neon spectral line 582.02 nm
For explanation see text

with neon pressure 364 Pa and the helium pressure 3296 Pa. Figure 6 also shows a fragment of the interferogram of reference tube (the source $K_3$) composed of a high frequency electrodeless discharge tube with pure neon at the pressure 120 Pa.

The figure 7 shows a plot of the half-width of the Lorentzian component of the 582.02 nm Ne I selfbroadened line on the neon pressure. Figure 7

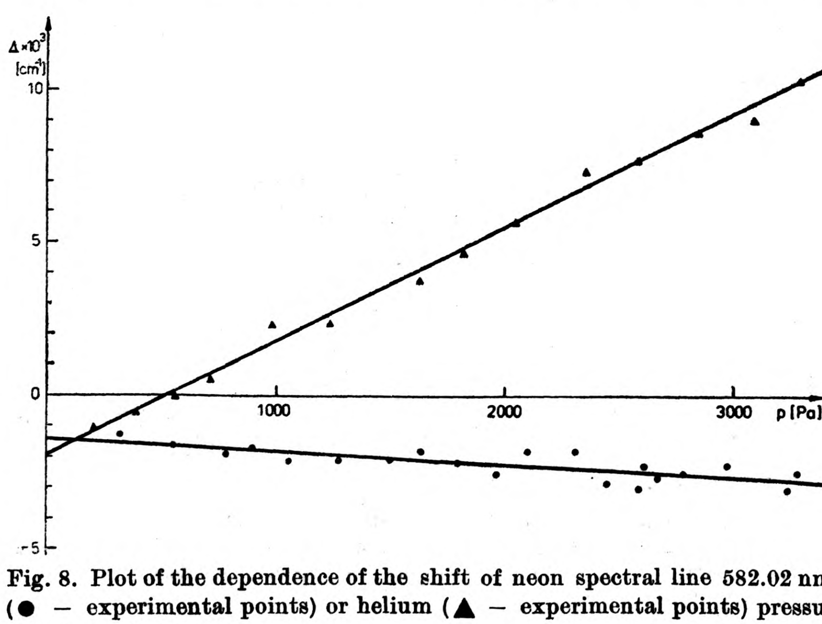


Fig. 8. Plot of the dependence of the shift of neon spectral line 582.02 nm on the neon (● — experimental points) or helium (▲ — experimental points) pressure
For explanation see text

also shows the dependence of the half-width of the same neon line emitted from a discharge in Ne–He mixture on the helium pressure at the constant neon pressure (364 Pa). The plot of the collision shift of the 582.02 nm Ne I line on the neon and helium pressure is shown in fig. 8.

The full report of our studies of collision effects on the 582.02 nm line of neon will be published elsewhere.

## Appendix

Although there might be a different versions of the control circuit working equally well, there are several critical points to which particular attention has to be paid of overall performance of the spectrometer is not to be seriously degraded.

In this section we discuss those points going somewhat deeper into details of our design.

As it has been mentioned in the previous sections, optical path length inside FPI is controlled by using long, approximately 1 m, Jamin interferometer with tube $R_2$ connected to the FPI chamber and tube $R_1$ open to the surrounding atmosphere — see fig. 1. It is very important that possibly short connecting tubes with small flow resistance between FPI chamber and Jamin interferometer be used, to avoid rapid change of the gas pressure inside interferometers, as well as to allow the relaxation of the transient phenomena, using appropriate time delay in the measuring sequence. It is also not recomended to work with gas pressure lower than about 6000 Pa. Disregard of those precautions can lead to significant pressure difference between FPI and Jamin interferometer, or pressure drifts during measurement cycle, seriously degrading linearity of the wavelength scale.

Under typical circumstances signal from the Jamin interferometer, as a function of the refraction index $\Delta\mu$, has the form shown in fig. 3. There is significant background signal $f_0$ caused by scattered light as well as some jitter in the cosecutive samples due to stochastic fluctuations and residual pressure drifts. At the same time the amplitude of the interference pattern remains quite constant within the whole spectral range covering the investigated line profile.

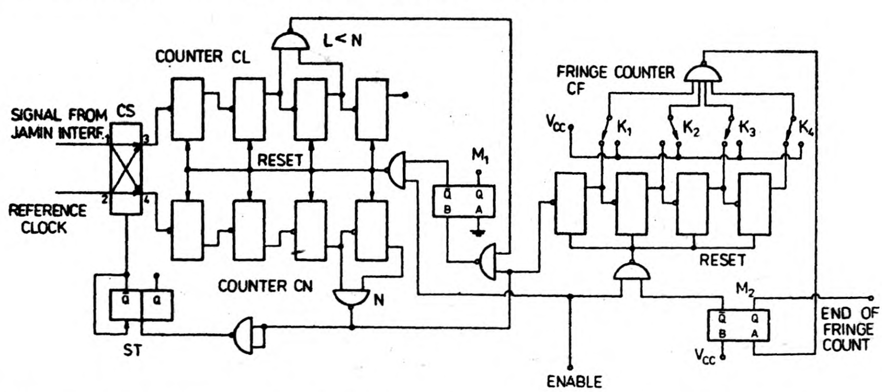


Fig. 9. Fringe counting circuit (simplified to essential components)

*CS* — change over gate, ports 1–4 2–3 or 1–3 2–4 are open depending on the logical states of ST trigger, $M_1$, $M_2$ — reset monoflops, *CN*, *CL* — integrating counters (only last four stages are shown), CF — fringe counter with programmed division ratio

In order to assure unambiguous fringe counting in the presence of the noise and occasional pressure fluctuation it is necessary to use two alternatively active discrimination levels $A$ and $B$ (see fig. 3). Actual implementation of this fringe counting principle, simplified to essentials is shown in fig. 9. In this circuit there are two integrating counters $CN$ and $CL$ with corresponding $N$ and $L$ division ratios. Depending upon logical state of the gate $CS$ controlled by the $ST$ trigger, counters $CN$ and $CL$ are counting respectively pulses from photomultiplier and from reference clock or just other way round. After accumulation of $N$ pulses in the counter $CN$ or $L$ pulses in the counter $CL$, a reset circuit is activated and both counters are cleared to zero. Each time when the counter $CN$ accumulates $N$ counts before the counter $CL$ accumulates $L$ counts a pulse is generated, changing logical state of the trigger $ST$ and advancing fringe counter $CF$ by one count. If $N$ nad $L$ are counters division ratio with $N > L$ and $f_c$ is reference clock frequency then, as it can be deduced from fig. 9, a fringe counter $CF$ is advanced each time when instantenous pulse frequency from Jamin interferometer $f_i$ fulfils alternately the following condition:

$$f_i \geqslant \frac{N}{L} f_c \quad \text{or} \quad f_i \leqslant \frac{L}{N} f_c$$

for the first time in each fringe period.

Referring to the fig. 3, fringe counter will be advanced twice in each fringe of the Jamin interferometer in the points $B_1, A_1, B_2, A_2, B_3$, respectively, and so on until fringe counter accumulates predefined number of counts. In the described spectrometer $N, L$ and $f_c$ were adjusted in such a way as to assure equal increments of the optical path length between points $B_1, A_1, B_2$, etc., corresponding to the half fringe from the Jamin interferometer. Unfortunately, under typical experimental conditions scattered light in the Jamin interferometer changes markedly if spectral range of the instrument is changed, which, in turn, upsets the proper adjustment of the discrimination levels $A$ and $B$. We found it advantageous to sophisticate a little more the fringe

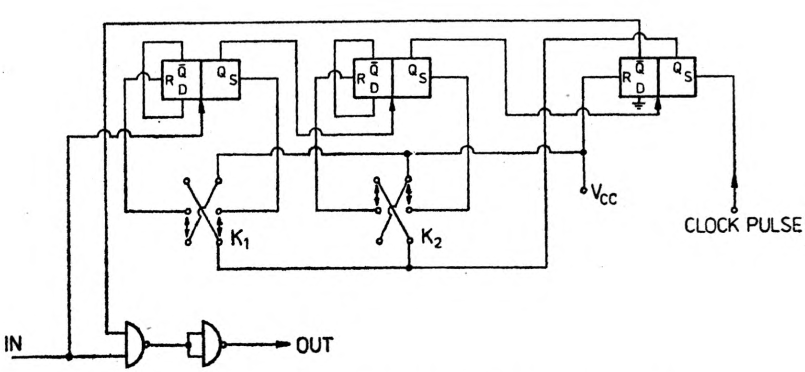


Fig. 10. Background signal subtraction unit (simplified to essentials)

counting circuit by adding a background substraction unit. Basic components of this unit are shown in fig. 10. Essentially this is a time gate which after each clock pulse remains closed for predefined number of input pulses. By varying the positions of keys $K_1, K_2, \dots K_n$ and adjusting properly clock frequency the background signal $f_0$ from Jamin interferometer can be reduced to the acceptable level. It is quite enough to adjust background compensation only once each time when spectral range of the spectrometer is changed.

*Acknowledgement* — The authors wish to express their gratitude to Dr. J. Szudy for reading the manuscript and for his helpful comments.

## References

[1] Bielski A., Kandela S. A., Wolnikowski J., Turło Z., Acta Phys. Polon. **A42** (1972), 295.
[2] Bielski A., Wolnikowski J., Acta Phys. Polon. **A54** (1978), 601.
[3] Bielski A., Lisicki E., Nesterov M., Wolnikowski J., Acta Phys. Polon. **A54** (1978), 611.
[4] Bielski A., Bierza S., Bystra K., Dokurno W., Physica **C97** (1979), 249.
[5] Lisicki E., Szudy J., Wolnikowski J., Acta Phys. Polon. **A55** (1979), 557.
[6] Alfano R. R., Ockman N., J. Opt. Soc. Am. **58** (1968), 90.

*Received April 26, 1980*

**Цифровой спектрометр с эталоном Фабри–Перо для иследования уширения и сдвига спектральных линий**

Описан автоматический сканированный давлением спектрометр с эталоном Фабри–Перо. Для контроля изменения давления с эталоном Фабри–Перо сопряжен интерферометр Жамена. Измерение сигнала проводится методом счёта фотонов.